

Cite this: *Nanoscale*, 2015, **7**, 13075

Therapeutic angiogenesis in ischemic muscles after local injection of fragmented fibers with loaded traditional Chinese medicine

Huiyan Li,^{†[a](#)} Huiying Wan,^{†[b](#)} Tian Xia,^c Maohua Chen,^a Yun Zhang,^a Xiaoming Luo^a and Xiaohong Li^{*[a](#)}

Therapeutic angiogenesis remains the most effective method to re-establish a proper blood flow in ischemic tissues. There is a great clinical need to identify an injectable format to achieve a well accumulation following local administration and a sustained delivery of biological factors at the ischemic sites. In the current study, fragmented nanofibers with loaded traditional Chinese medicines, astragaloside IV (AT), the main active ingredient of astragalus, and ferulic acid (FA), the main ingredient of angelica, were proposed to promote the microvessel formation after intramuscular injection into ischemic hindlimbs. Fragmented fibers with average lengths of 5 (FF-5), 20 (FF-20) and 80 µm (FF-80) were constructed by the cryocutting of aligned electrospun fibers. Their dispersion in sodium alginate solution (0.2%) indicated good injectability. After injection into the quadriceps muscles of the hindlimbs, FF-20 and FF-80 fiber fragments showed higher tissue retentions than FF-5, and around 90% of the injected doses were determined after 7 days. On a hindlimb ischemia model established by ligating the femoral arteries, intramuscular injection of the mixtures of FA-loaded and AT-loaded FF-20 fiber fragments substantially reduced the muscle degeneration with minimal fibrosis formation, significantly enhanced the neovessel formation and hindlimb perfusion in the ischemic tissues, and efficiently promoted the limb salvage with few limb losses. Along with the easy manipulation and lower invasiveness for *in vivo* administration, fragmented fibers should become potential drug carriers for disease treatment, wound recovery and tissue repair after local injection.

Received 29th March 2015,
Accepted 15th June 2015
DOI: 10.1039/c5nr02005k
www.rsc.org/nanoscale

1. Introduction

Ischemia is a severe medical condition resulting from the obstruction of blood flow and is becoming a leading cause of morbidity and mortality in Western societies. Peripheral arterial disease (PAD) is a common disorder caused by occlusive atherosclerosis in a vascular bed other than the heart, and usually leads to ischemic pain and ulcers in the lower extremities due to the lack of oxygen and nutrients. Critical limb ischemia (CLI) is a severe clinical manifestation of PAD, wherein reduced blood perfusion leads to the ischemic necroses of the surrounding muscular and fibrous tissues and the risk of limb amputation in severe conditions.¹ Clinical

observations indicated that less than 20% of CLI patients are eligible for mechanical revascularization therapies, such as invasive surgical interventions and stent implantation, to re-establish a proper blood flow in the underperfused regions. The only hope for the remaining patients lies in therapeutic angiogenesis to salvage their ischemic limbs.² Therapeutic angiogenesis aims to build new blood vessels in ischemic tissues *via* sprouting and branching from existing vessels, currently involving cell transplantation, growth factor administration or a combination of cell and cytokine therapies.³ The transplantation of bone marrow mononuclear cells, mesenchymal stem cells or endothelial progenitor cells has been developed to form vessel networks for the treatment of ischemic diseases.⁴ However, over two thirds of the transplanted cells were estimated to disappear from the injection site within 1 week of transplantation.⁵ In addition, the cell-based therapy suffers from low rates of cell survival, potential tumorigenesis, and donor cell shortage.⁶

The use of angiogenic factors, such as growth factors, cytokines, and plasmid DNA-encoding angiogenic factors has been explored in the treatment of limb ischemia or myocardial infarction.⁷ Kato *et al.* examined the effect of erythropoietin

^aKey Laboratory of Advanced Technologies of Materials, Ministry of Education of China, School of Materials Science and Engineering, Southwest Jiaotong University, Chengdu 610031, P. R. China. E-mail: xhli@swjtu.edu.cn; Fax: +86 28-87634649; Tel: +86 28-87634068

^bDepartment of Dermatology, Sichuan Provincial People's Hospital, Chengdu 610031, P. R. China

^cDepartment of Pathology, The 452nd Hospital of People's Liberation Army, Chengdu 610021, P. R. China

†The authors contributed equally to the work.

administration in a mouse model of acute hindlimb ischemia, indicating an enhancement of blood flow recovery and vessel densities in the ischemic tissues.⁸ Current cytokine therapy primarily relies on a bolus administration and faces major hurdles, such as the short half-life and transit function of growth factors and the variable transfection efficiency of genes to target cells.⁹ In addition, an over-dose or over-expression of the factors may lead to various unwanted side effects, for example, fragile and leaky vessels that were prone to regression.¹⁰ Therefore, a great deal of attention has been given to the design of appropriate carriers to facilitate the protection and sustained release of biological factors in target sites.¹¹ Chappell *et al.* delivered poly(D,L-lactic-co-glycolic acid) (PLGA) nanoparticles containing basic fibroblast growth factor (bFGF) to mouse muscles with hindlimb arterial insufficiency, indicating a significant increase in both the caliber and total number of collateral arterioles after two weeks of treatment.¹² However, the injection of micro- or nanoparticle suspensions indicated a quick migration of these particles from the administration site.¹³ Alternatively, Zhou *et al.* designed a complex of collagen matrix and bFGF, showing that the formation of capillaries and mature vessels was significantly enhanced after intramuscular implantation into a rabbit ischemic model.¹⁴ However, the physical implants require direct accessibility through surgical procedures, having a large invasiveness. Therefore, *in situ* gelling systems have been proposed with the aim of being applied for minimally-invasive drug delivery. Daugherty *et al.* prepared a gel of PLGA solubilized in *N*-methyl pyrrolidone loaded with vascular endothelial growth factor, indicating that the local injection to peripheral ischemia sites achieved a sustained release of this potent mitogen and a durable benefit in the context of PVD.¹⁵ However, the injectability and gelation process should be balanced in the *in situ* gelling system, wherein the diffusion of organic solvents before gelation and their retention after gelation showed potential effects on the biocompatibility of these systems.¹⁶ Therefore, it is essential to identify an injectable format to achieve a well retention following local injection and a sustained delivery of biological factors at the ischemic sites.

Traditional Chinese medicine is another type of a biological factor that promotes vascularization and is gradually being accepted by more people worldwide due to its effectiveness, weak side effects, and safety.¹⁷ In a previous study, astragaloside IV (AT), the main active ingredient of astragalus, and ferulic acid (FA), the main ingredient of angelica, were loaded into electrospun fibrous scaffolds to provide abundant and sustained biological factors. The cell proliferation after AT and FA treatment was dose-dependent, and the electrospun fibers containing AT and FA with the ratio of 7:3 demonstrated the most significant angiogenesis promotion.¹⁸ Electrospinning affords great flexibility in loading antibiotics, anticancer drugs, proteins, and DNA into ultrafine fibers, and electrospun fibers have been shown to be effective for the local and sustained delivery of bioactive signals due to its interconnected pores and high specific surface areas.¹⁹ However, fibers need to be implanted into tissues, meaning a high invasiveness. In

the current study, fragmented fibers were initially constructed with the loading of AT and FA to promote the microvessel formation after intramuscular injection into the ischemic hindlimbs. Fragmented fibers not only retain the advantages of continuous fibers, such as large specific surface areas and localized and controlled drug delivery, but also provide an injectability to reduce the invasion of tissues. Fragmented fibers were constructed by cryocutting of aligned, electrospun fibers and their lengths could be conveniently controlled by adjusting the slice thickness. The lengths of fiber fragments were optimized in the current study to achieve a good injectability and tissue retention after local injection. In addition, the injection of mixtures of AT-loaded and FA-loaded fiber fragments was proposed to easily modulate the dose ratios of AT and FA, providing the maximal synergistic promotion of blood vessel regeneration. On a hindlimb ischemia model established by ligating the femoral arteries, the improvement of ischemic recovery was determined by physiological status evaluation, blood perfusion monitoring, and histological and immunohistochemical analyses of quadriceps muscles retrieved.

2. Materials and methods

2.1. Materials and cells

Poly(ethylene glycol)-poly(DL-lactide) (PELA, $M_w = 50$ kDa, $M_w/M_n = 1.23$) was prepared by the bulk ring-opening polymerization of lactide/poly(ethylene glycol) using stannous chloride as the initiator.²⁰ Polystyrene (PS, $M_w = 280$ kDa), coumarin 6, bovine serum albumin (BSA), dimethyl sulfoxide (DMSO), 2,3,5-triphenyltetrazolium chloride (TTC) and dialysis membrane (1 and 3.5 kDa cutoff) were obtained from Sigma-Aldrich (St. Louis, MO). AT and FA of over 99% purity were purchased from the National Institutes for the Control of Pharmaceutical and Biological Products (Beijing, China). Rabbit anti-human antibodies of collagen I, collagen IV, laminin, α -smooth muscle actin (α -SMA) and β -actin; rabbit anti-mouse antibodies of CD31, collagen IV and α -SMA; and goat anti-rabbit IgG-fluorescein isothiocyanate (FITC), IgG-horseradish peroxidase (HRP) and 3,3'-diaminobenzidine (DAB) developer were purchased from Boster Bioengineering Co. Ltd (Wuhan, China). All other chemicals were of analytical grade and received from Changzheng Reagent Company (Chengdu, China), unless otherwise indicated. Endothelial cells (ECs) were isolated from freshly obtained human umbilical cords by the collagenase digestion of the interior of veins,²¹ while smooth muscle cells (SMCs) were obtained by outgrowth from the discarded pieces of umbilical arteries as described previously.²² ECs and SMCs were expanded in Dulbecco's modified Eagle's medium (DMEM, Gibco BRL, Rockville, MD) supplemented with 10% heat-inactivated fetal bovine serum (FBS, Gibco BRL, Grand Island, NY).

2.2. Preparation of drug-loaded fiber fragments

Drug-loaded fiber fragments were obtained by cryocutting aligned electrospun fibers, which were prepared as described

elsewhere.²³ Briefly, PELA and AT (or FA) were dissolved in DMSO and transferred to a 5 mL syringe attached to a blunt metal needle as the nozzle. A steady flow out of the nozzle was controlled at 2.0 mL h⁻¹ by a microinject pump (Zhejiang University Medical Instrument Co., Hangzhou, China). A high voltage difference of 20 kV was applied between the nozzle and a grounded collector through a high voltage statitron (Tianjing High Voltage Power Supply Co., Tianjing, China). A drum with a diameter of 30 cm was used as the collector, which was rotated with a linear rate of around 15 m s⁻¹ to collect the aligned fibers.²³ After vacuum-drying at room temperature for 2 days to remove the remaining organic solvent, the collected fibers were folded vertically to about 1 cm in length and placed parallel to each other in a plastic embedding cryomold (Fig. 1a). After the addition of Cryo-OCT compound (Thermo Fisher Scientific Inc., Waltham, MA), the mold was frozen at -70 °C for 5 min, resulting in a solidified block of gel with fibrous mats embedded therein. The blocks were sectioned using a cryostat microtome (Microme HM550 OMC, Thermo Fisher Scientific Inc., Waltham, MA) at -20 °C with the section thickness of 5, 20, and 80 µm, which were used to prepare fragmented fibers of FF-5, FF-20, and FF-80, respectively. The fiber bundles were harvested in water and separated into individual fiber fragments after ultrasonication for 5 min. The fragmented fibers were harvested in water and separated into individual fiber fragments after ultrasonication for 5 min. The fragmented fibers were collected by centrifugation and freeze-dried.

Fragmented PS fibers loaded with 0.1% of coumarin 6 (PS/C6) were prepared using the same procedures. For comparison, electrospun fibers with the encapsulation of both AT and FA (EF – A/F) with the weight ratio of 7 : 3 were also prepared as described previously.¹⁸

2.3. Characterization of drug-loaded fiber fragments

The morphologies of electrospun fibers and fragmented fibers were investigated by a scanning electron microscope (SEM, FEI Quanta 200, the Netherlands) equipped with a field-emission gun (20 kV) and a Robinson detector after 2 min of gold coating to minimize the charging effect. The morphology of electrospun and fragmented PS/C6 fibers was observed by a fluorescence microscope (Olympus IX51-FL, Japan). From each SEM image, at least 20 different fibers and 200 different segments were randomly selected and their diameters were measured to generate an average size using Photoshop 10.0 edition. SEM images with the magnification of 2000 and at least 20 different fibers from each image were randomly chosen to obtain the fiber orientation, which was analyzed by measuring the individual orientation and angular deviation of fibers as described previously.²³ The average length of fragmented fibers was determined using at least 100 fragmented fibers from the optical and SEM images.

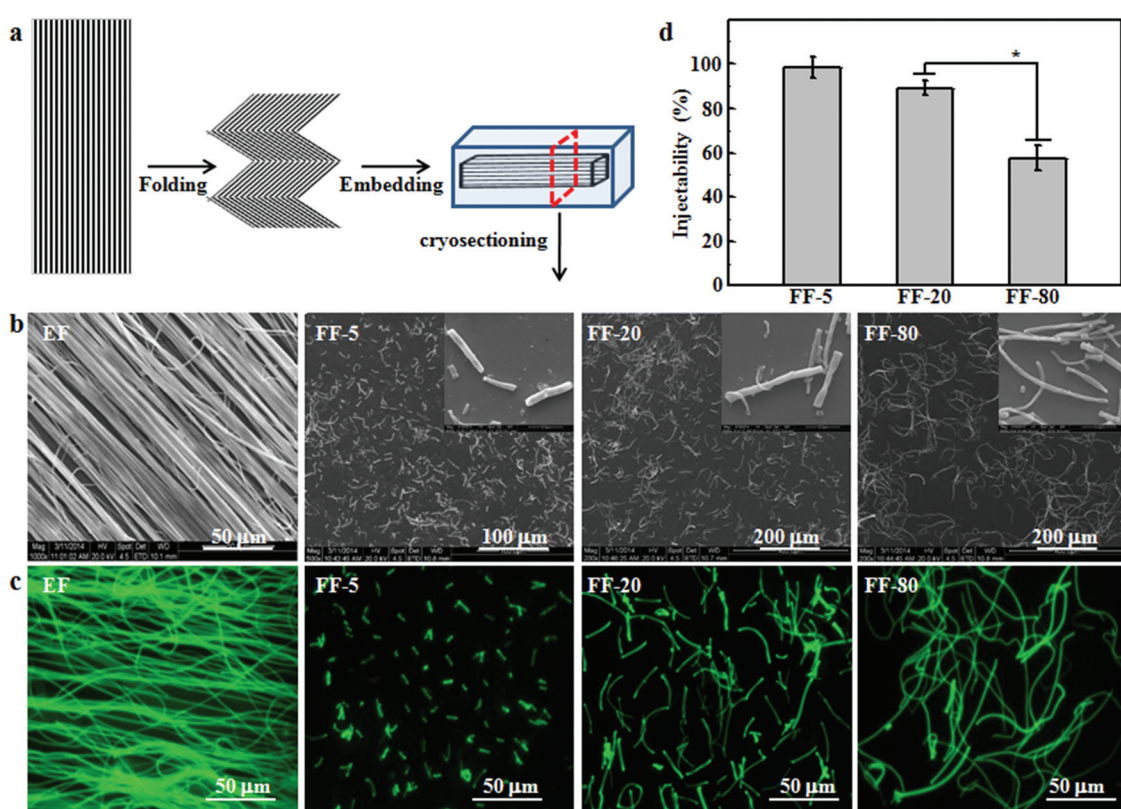


Fig. 1 (a) Schematic of the preparation process of fragmented fibers. (b) Typical SEM and (c) fluorescence microscope images of electrospun aligned fibers, FF-5, FF-20 and FF-80 fiber fragments. (d) Injectability of FF-5, FF-20 and FF-80 fiber fragments dispersed in sodium alginate solution, determined from the amount of fiber fragments injected out of 26G1/2 syringe needles in comparison with that used for testing ($n = 4$, * $p < 0.05$).

The loading amount and encapsulation efficiency of AT and FA in electrospun and fragmented fibers were determined after extraction with phosphate buffered saline (PBS) as described previously.¹⁸ Briefly, a known amount of fibers (*ca.* 2 mg) was dissolved in 500 µL of chloroform and extracted three times with 2.5 mL of pH 7.4 PBS. The amount of AT in the extract was measured using a fluorescence spectrophotometer (Hitachi F-7000, Japan) with the excitation wavelength of 310 nm and the emission wavelength of 376 nm²⁴ and that of FA using a UV spectrophotometer (Shimadzu UV2550, Japan) at the wavelength of 310 nm.²⁵ The drug concentrations were obtained using a standard curve from known concentrations of AT and FA solutions, and the extraction efficiency was calibrated by adding a certain amount of drug into the polymer/chloroform solution along with the same concentration as mentioned above and extracting using the abovementioned process. The drug loading amount indicated the amount (in milligrams) of drug encapsulated per 100 mg of fibers. Furthermore, the encapsulation efficiency was obtained by comparing the amount of drug encapsulated to the total amount used for fiber preparation. The loading amount of coumarin in electrospun and fragmented PS fibers was determined by the fluorescence spectrophotometer with the excitation wavelength of 460 nm and the emission wavelength of 505 nm following the same procedures.

The injectability of fragmented fibers was determined as described previously with some modifications.²⁶ Briefly, 20 mg of fragmented fibers were dispersed homogeneously into 2 mL of sodium alginate solution in PBS (2%, v/v) and transferred to a 5 mL syringe. A 26G1/2 syringe needle with the inner nozzle size of 0.25 mm was held straight downwards and a constant pressure of 1.2 N was applied on the top of the syringe piston by a fixed object. The suspension of fragmented fibers was harvested during 40 s of injection out of syringe, followed by centrifugation and freeze-drying. The injectability is indicated by the amount of fragmented fibers collected after injection compared with that used for testing.

2.4. *In vitro* drug release from fiber fragments

The drug release profiles were determined from the fragmented fibers of different lengths using electrospun fibers as the control. Briefly, 20 mg of fragmented fibers with loaded AT, FA or coumarin were dispersed in 1 mL of PBS and transferred into dialysis bags (3.5 kDa cutoff). The dialysis bags were placed into a conical tube and immersed in 20 mL of PBS to ensure a sink condition. All the tubes were placed in a thermostated shaking water bath that was maintained at 37 °C and 100 cycles per min. At predetermined time intervals, 1.0 mL of the release buffer was removed for analysis and fresh PBS was added for continued incubation. The concentrations of AT, FA and coumarin in the release media were detected as described above. The percentage drug release against incubation time was determined from the amount of accumulated release into the media compared with the amount of drug loaded in the fibers.

2.5. Cell proliferation after treatment with drug-loaded fiber fragments

The influence of drug-loaded electrospun fibers and fiber fragments of different lengths on the growth of primary ECs and SMCs was evaluated by CCK-8 assay as described previously.¹⁸ Briefly, electrospun and fragmented fibers were sterilized by electron-beam irradiation using a linear accelerator (Precise, Elekta, Crawley, UK) with a total dose of 80 cGy. EC or SMC suspensions were seeded into a 48-well tissue culture plate (TCP) at a density of 5×10^3 cells per well. After incubation with 100 µL of DMEM supplemented with 10% FBS for 24 h, the media were removed and replenished by 100 µL of culture media containing EF – A/F fibers or mixtures of AT-loaded and FA-loaded fiber fragments. The doses of AT and FA were 0.14 and 0.06 mg mL⁻¹, respectively, for electrospun and fragmented fibers of different lengths. At predetermined intervals, the fiber-containing media were removed, followed by the addition of 200 µL fresh culture medium and 20 µL CCK-8 reagent (Dojindo Molecular Technologies Inc., Kumamoto, Japan) into each well. After incubation for 2 h according to the reagent instruction, 100 µL of the incubation medium was pipetted into another 96-well TCP and the absorbance of each well was measured at 450 nm using a µQuant microplate spectrophotometer (Elx-800, Bio-Tek Instrument Inc., Winooski, VT). The cell proliferation test was repeated on day 1, 3, and 5 after incubation.

2.6. Matrix synthesis of cells after treatment with drug-loaded fiber fragments

The expression of collagen IV and laminin by ECs and that of collagen I and α-SMA by SMCs were observed after immunofluorescent staining as described previously.¹⁸ Briefly, cells were cultured as mentioned above on coverslips in a 24-well TCP, and media containing fibers were removed after 5 days. Cells were fixed with 10% buffered formaldehyde and permeabilized with 0.1% Triton X-100 solution in PBS. After blocking by incubation with 2% BSA for 30 min at 37 °C, cells were incubated with rabbit anti-human antibodies of collagen I, collagen IV, laminin, or α-SMA for 2 h at 37 °C. After washing three times with PBS, samples were incubated with goat anti-rabbit IgG–FITC in the dark for 1 h at 37 °C. The cells were then mounted and observed using a confocal laser scanning microscope (CLSM, Leica TCS SP2, Germany) with the excitation and transmission wavelengths of 488 and 535 nm, respectively.

2.7. *In vivo* distribution of fragmented fibers after local injection

All animal procedures were approved by the University Animal Care and Use Committee. In order to evaluate the retention of fragmented fibers of different lengths in muscles, fragmented PS/C6 fibers were suspended in sodium alginate solution and injected into the left hindlimb of nude mice (aged 8 weeks, Sichuan Dashuo Biotech Inc., Chengdu, China). The injection was performed at 4 locations in the quadriceps muscles at a

dose of 5 mg coumarin per kg body weight. The mice were anesthetized and imaged by a Maestro *In vivo* Imaging System (Maestro EX-Pro, PerkinElmer, Waltham, MA) at the excitation wavelength of 460 nm and the emission wavelength from 500 to 750 nm. Then, the mice were sacrificed and the liver, spleen, heart, lung, and quadriceps muscles were harvested for imaging as mentioned above.

In order to quantify the tissue distribution, fiber fragment suspensions were locally injected into the quadriceps muscles of Balb/C mice (Sichuan Dashuo Biotech Inc., Chengdu, China) as mentioned above. The mice were sacrificed after injection for 7 and 28 days to retrieve tissues, such as quadriceps muscles, liver, spleen, kidneys, limb lymph nodes, and lung, which were homogenized with saline. The fluorescence intensities of coumarin in the tissue homogenate were measured with a fluorescence spectrophotometer as mentioned above. The amount of fragmented fibers in a tissue was obtained using a standard curve from known concentrations of fragmented PS/C6 fibers in the homogenate of this tissue from untreated mice. The percentage of injected dose (ID%) indicated the ratio of the actual amount of fiber in a tissue to the total amount of injected fiber, and the percentage dose rate (ID% per g) was used to represent the fiber accumulation per gram of a tissue.²⁷

2.8. Treatment of hindlimb ischemia by the injection of drug-loaded fiber fragments

The hindlimb ischemia model was established by ligating the left femoral arteries as described previously.²⁷ Briefly, Balb/C mice were anaesthetized by the intraperitoneal injection of pentobarbital at 30 mg kg⁻¹, and hair on the thighs and groins of the two hindlimbs was removed with a depilatory cream. A 15 cm long incision was made on the left medial thigh to expose the deep femoral artery below the neurovascular bundle and above the collateral arteries. Both the proximal and distal portions of the femoral artery were ligated with 7–0 silk suture, and the segment between the ligature and its branches were excised using microscissors. After suturing the incisions, the animals were allowed to recover under a heating pad.

One day after surgery, the mice were randomly divided into five experimental groups. Animals were treated with mixtures of AT-loaded and FA-loaded fragmented fibers (FF – A/F), mixtures of fragmented fibers with free AT and FA (FF + A/F), and fragmented fibers without drug entrapment (FF), using saline injection as the control. Fragmented fibers were suspended in 100 µL of sodium alginate solution in PBS (2%, w/v) and injected at 4 locations in the ischemic zone by 26G1/2 needles. For comparison, electrospun EF – A/F fibers were implanted in the ischemic zones after surgery. The doses of AT and FA for all the groups were 35 and 15 mg per kg body weight, respectively.

2.9. Treatment efficacy for the hindlimb ischemia

The physiological status of the ischemic hindlimbs was observed for 4 weeks after treatment, and the symptoms were divided into three levels for quantitative analysis: limb loss

(necrosis or loss of tissues above the ankle), foot necrosis (necrosis of toes, but not above the ankle), and limb salvage (almost all toes of an ischemic hindlimb maintained).²⁸

The blood flow in the two hindlimbs was measured using a laser Doppler perfusion (LDP) monitor (PeriFlux System 5000, Perimed AB, Järfälla, Sweden) prior to and right after surgery, and after treatment for 1, 3, 7, 14, and 28 days as described previously.²⁹ Briefly, the measurement was performed on six different locations on each leg, and the mean value of blood perfusion was used to evaluate the blood flow. The perfusion ratio was expressed as the blood flow of the ischemic hindlimb compared with that of the normal one in the same animal. The rectal temperature was maintained at 37 ± 0.5 °C using a thermistor-controlled heating blanket during measurement.

To identify the morphological differences among ischemic muscles in each group, the retrieved muscles were stained with TTC as described previously.³⁰ Briefly, the muscles in the ischemia zone were retrieved after treatment for 28 days and cut into slices of 2 mm thick, followed by incubation for 30 min in 2% TTC solution. The stained muscles were photographed after fixation for 30 min in 10% buffered formaldehyde.

2.10. Histological and immunohistochemical analyses

The quadriceps muscles of test animals were harvested after treatment for 7 and 28 days. The retrieved muscles were fixed in 10% buffered formaldehyde, paraffin-embedded, sectioned into 4 µm-thick slices, and processed for histological analyses. Hematoxylin and eosin (HE) staining was performed routinely on tissue sections, and observed with a light microscope (Nikon Eclipse E400, Japan) to identify muscle degeneration and tissue inflammation.³¹ The tissue sections were also stained with a Masson's Trichrome staining kit (BBC Biochemical, Stanwood, WA) to examine fibrosis formation in the ischemic region. Ten images were randomly captured by a light microscope, and the percentage of fibrosis was calculated as the area ratio of muscle (red) to fibrosis (blue) using the Image-ProPlus software.³²

The densities of capillaries and arterioles in the ischemic tissues were quantified after immunohistochemical assessment of CD-31 and SMA expressions in retrieved muscles as described previously.³³ Briefly, serial sections were exposed under 3% H₂O₂ for 10 min to inactivate endogenous peroxidase, followed by incubation with 10 mM citrate buffer solution (pH 6.0) to recover antigens. After treatment with 5% BSA in Tris-buffered saline for 20 min to block nonspecific binding sites, the sections were incubated with primary antibodies of CD-31 or SMA at 4 °C overnight, followed by exposure under secondary antibody IgG-HRP for 20 min. The antibody binding sites were visualized by incubation with a DAB-H₂O₂ solution. The slides were counterstained for 1 min with hematoxylin and then dehydrated with sequential ethanol for sealing and microscope observation. The number of microvessels was counted in 20 randomly selected optical fields from 5 different transverse sections for each sample, and normalized to the areas (mm²) of these fields.³⁴

2.11. Statistics analysis

The results are reported as mean \pm standard deviation (SD). An appropriate comparison among multiple groups was performed by the analysis of variance (ANOVA), while a two-tailed Student's t-test was used to discern the statistical difference between the two groups. A probability value (p) of less than 0.05 was considered to be statistically significant.

3. Results and discussion

3.1. Characterization of drug-loaded fiber fragments

Fig. 1a shows the cryocutting process of electrospun fibers, which were collected on a high-speed rotating collector. Electrospun fibers were obtained with high alignment and uniform morphology, and only few fibers showed significant angular deviation (Fig. 1b). The rapid deposition of fibers on the grounded collector offered insufficient time to completely release the charge, resulting in the repulsion of fibers depositing and those deposited.²³ Aligned fibers indicate an orientation degree of $91.4 \pm 3.5\%$ and an average diameter of $0.97 \pm 0.3 \mu\text{m}$. As shown Fig. 1b, through controlling the section thickness, average lengths of 7.1 ± 2.2 , 22.9 ± 5.1 and $76.4 \pm 14.4 \mu\text{m}$ were determined for FF-5, FF-20 and FF-80 fiber fragments, respectively. Efficient drug encapsulation was one of the advantages of electrospun fibers,³⁵ and a drug loading efficiency of over 95% was achieved in the current study. The loading amounts of AT and FA in fragmented fibers were 1.4% and 0.6%, respectively, and EF – A/F fibers indicated a drug loading content of 1.0% with an AT/FA ratio of 7/3.

Injectability is crucial for the local application of fragmented fibers, and a good flow property is necessary to ensure dose uniformity and safety requirements. In the current study, sodium alginate solution (2%, w/v) was used to suspend fiber fragments to achieve a homogenous dispersion. Sodium alginate is a wetting and biocompatible agent, and commonly used as a viscosity-building agent in the formulation of oral and injectable pharmaceutical suspensions.³⁶ All the fibers were injected out smoothly through syringe needles, and the injectability of fragmented fibers was determined by comparing the amount of fibers injected out during 40 s. As shown in Fig. 1d, FF-5 and FF-20 fiber fragments showed a significantly better injectability than FF-80.

3.2. Drug release profiles from fragmented fibers

Fig. 2 shows the percentage release of AT and FA from EF – A/F fibers and fragmented fibers of different lengths. All the fragmented and electrospun fibers indicated similar release profiles containing three phases: an initial burst release of around 15% during 24 h, a sustained and quick release of an additional 45% during around 1 week, followed by a gradual release for about 3 weeks. As shown in Fig. 2a and b, there was around 78.8% of AT and 83.5% of FA released from EF – A/F fibers during 25 days of incubation. The similar release profiles of AT and FA indicated that there were sufficient sites within fibers available for drug loading, and no interference of

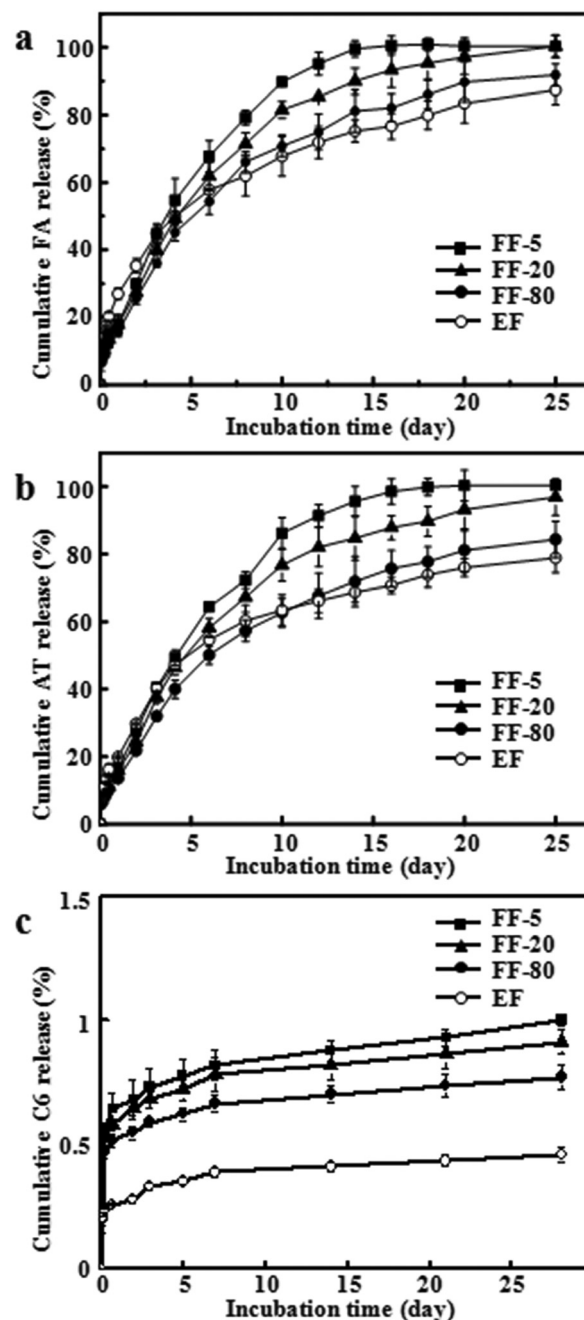


Fig. 2 (a) Percent release of FA, (b) TA and (c) coumarin 6 from electrospun fibers, FF-5, FF-20 and FF-80 fiber fragments after incubation at 37 °C in PBS ($n = 3$).

their co-loadings of AT and FA in fibers on the drug release rate. As shown in Fig. 2a, there was around 18.1%, 17.9%, and 15.6% of FA release during 1 day of incubation with FF-5, FF-20, and FF-80 fiber fragments, respectively. After incubation for 25 days, a complete release was observed for FF-5 and FF-20 fiber fragments, while FF-80 indicated about 91.8% of accumulated release. Similar release profiles were determined for AT release from fragmented fibers of different lengths (Fig. 2b). It was shown that the release rate was slightly higher

for shorter fragmented fibers, due to the increased release from the cross sections. In addition, the similar release profiles of AT and FA from fragmented fibers suggested that the doses of AT and FA could be easily modulated from the mixture of AT-loaded and FA-loaded fiber fragments.

3.3. Growth behaviours and matrix syntheses of cells after treatment with drug-loaded fiber fragments

In the previous study, the sustained release of AT and FA from electrospun fibers stimulated the cell growth and induced significantly high densities of vascular structures after subcutaneous implantation, compared with fibers without drug entrapment and in the presence of free drugs.¹⁸ Thus, in the current study, the proliferation of ECs and SMCs were compared after incubation with drug-loaded fragmented fibers of different lengths. Depending on the drug loading content and release profiles from fragmented and electrospun fibers, FA-loaded and AT-loaded fiber fragments were mixed together to achieve the same dose and ratios of AT and FA as those of EF – A/F. As shown in Fig. 3a and b, after incubation for 5 days, all the fiber samples indicated around 2.5-fold and 2.2-fold higher cell proliferation of ECs and SMCs, respectively, compared with TCP. There was no significant difference in the cell

proliferation enhancement among fragmented fibers of different lengths and EF – A/F ($p > 0.05$).

The extracellular matrix (ECM) synthesis is an important step for the generation of functional tissues. In the current study, the expression of collagen IV and laminin were evaluated on ECs, which play a central role in the production of a basal lamina in the microvessel formations.³⁷ Fig. 3c shows the immunofluorescent staining images of collagen IV expressions by ECs with a cobblestone-like morphology. Similar results were obtained for immunofluorescent staining of α -SMA by SMCs (Fig. 3d), wherein the expressions of smooth muscle-specific variants of cytoskeletal and contractile proteins were the substantial function of vascular SMCs to maintain the integrity and function of mature blood vessels.³⁸

3.4. Tissue distribution of fragmented fibers after local injection

In order to evaluate the disposition in the quadriceps muscles after local injection, fragmented PS/C6 fibers of different lengths were prepared. PS fibers were selected because they are not biodegradable, thus enabling the evaluation of the temporal biodistribution without resorption as a confounding variable. Fig. 1c shows the fluorescence microscope images of

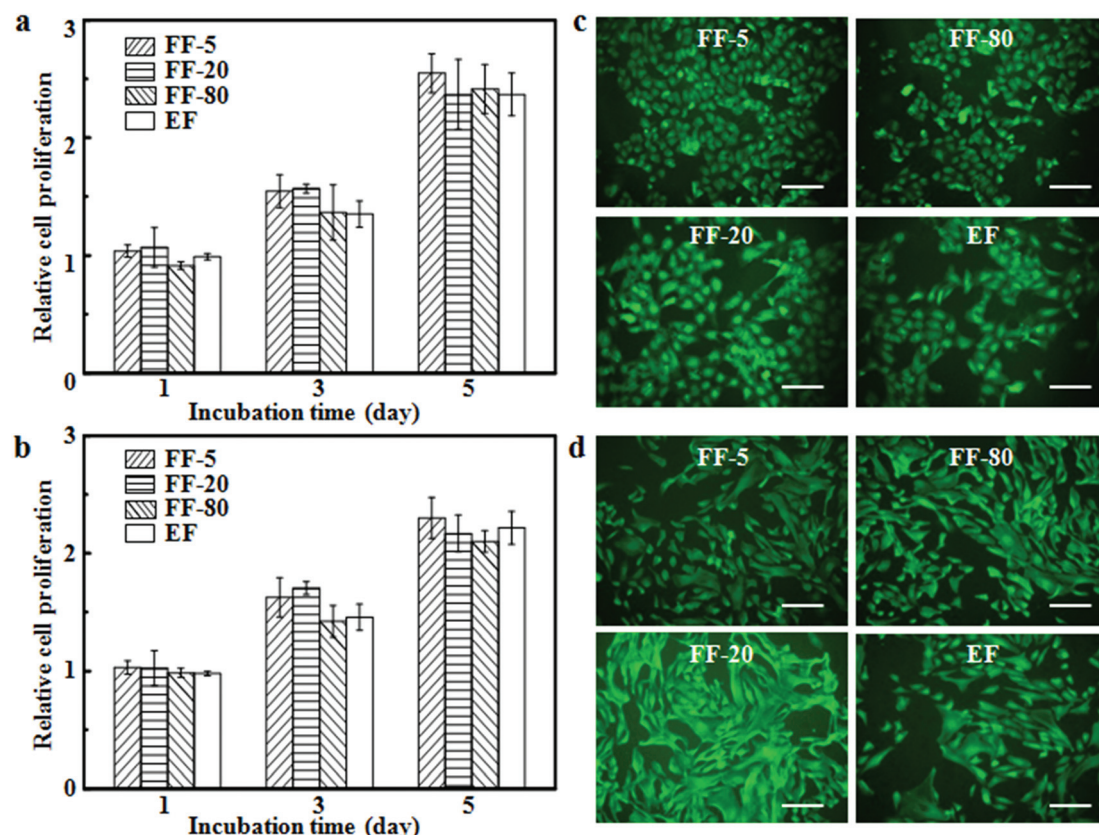


Fig. 3 (a) The proliferation of ECs and (b) SMCs after incubation for 1, 3 and 5 days with the mixtures of AT-loaded and FA-loaded fiber fragments of FF-5, FF-20 and FF-80, and electrospun fibers with AT and FA loaded, compared with that of TCP. The doses of AT and FA were 0.14 and 0.06 mg mL⁻¹, respectively ($n = 6$). (c) Immunofluorescent staining images of collagen IV expressions by ECs and (d) α -SMA by SMCs after incubation for 5 days with drug-loaded fragmented and electrospun fibers. Bars represent 20 μ m.

electrospun PS/C6 fibrous mats and fragmented fibers. Highly aligned fibers with an average diameter of $0.89 \pm 0.14 \mu\text{m}$ were obtained, and FF-5, FF-20 and FF-80 fiber fragments indicated average lengths of 7.2 ± 2.5 , 22.7 ± 5.3 and $80.1 \pm 16.7 \mu\text{m}$, respectively. The coumarin loading amount was only 0.1%, and a minimal coumarin leakage was crucial for an efficient tracking efficiency and low toxicity during *in vivo* evaluation. As shown in Fig. 2c, less than 1% of the coumarin loaded was released from fragmented fibers of different lengths, and less than 0.5% of release was observed after the initial release period. It was indicated that fragmented PS/C6 fibers could be used in the subsequent *in vivo* retention tests, and the signals of coumarin fluorescence could be taken to represent the fiber retention.

To directly visualize the retention of fragmented fibers after local injection into the quadriceps muscles of left hindlimbs, nude mice were imaged *in vivo* after 7 days. As shown in Fig. 4a, strong and clear bioluminescence signals were detected at the hindlimb, and stronger intensities were detected for FF-20 and FF-80 fiber fragments than for FF-5. The mice were then sacrificed to retrieve quadriceps muscles as well as liver, heart, spleen, lung, and kidney, and these imaged. As shown in Fig. 4b, most of the fragmented fibers were retained in the muscles, and FF-20 and FF-80 fiber fragments indicated higher tissue retention than FF-5.

In order to quantify the distribution of fragmented fibers of different lengths, the fluorescence intensities of coumarin were determined after 7 and 28 days in such tissues as liver, kidneys, spleen, lungs, limb lymph nodes and quadriceps muscles. In addition to muscles, only in the liver, spleen and

lungs, the existence of PS/C6 fiber fragments was detected after injection for 7 and 28 days, and the fluorescence intensities in the kidneys and limb lymph nodes were undetectable. As shown in Fig. 4c and d, significantly higher amount of fibers remained per gram of quadriceps muscles than those of other tissues ($p < 0.05$). In addition, after normalizing with the weight of tissues, around 76.8%, 89.9%, and 98.3% of FF-5, FF-20, and FF-80 fiber fragments were detected in the quadriceps muscles after 7 days, respectively, and there were significant differences among the groups ($p < 0.05$). A similar retention profile was detected after 28 days, at around 60.4%, 77.5%, and 84.5% of injected doses for FF-5, FF-20, and FF-80 fiber fragments, respectively (Fig. 4d). Most of the fiber fragments were retained in the ischemic hindlimbs following injection, and increasing the length of fragmented fibers could reduce the exposure of therapeutic agents to non-target sites, by hindering the transport through lymphatic and venous vessels.

As indicated above, FF-5, FF-20 and FF-80 fiber fragments had a similar release profile for both AT and FA (Fig. 2), and the promotion of cell proliferation and ECM syntheses showed no significant difference among the fragmented fibers (Fig. 3). The injectability of FF-5 and FF-20 fiber fragments was significantly higher than that of FF-80 (Fig. 1), but FF-20 and FF-80 showed higher tissue retention in the ischemic hindlimbs than FF-5 (Fig. 4). Considering the effect of fiber lengths on the injectability, drug release profiles, cell proliferation, and tissue distributions, FF-20 fiber fragments with loaded AT and FA were used to treat hindlimb ischemia after local injection into quadriceps muscles.

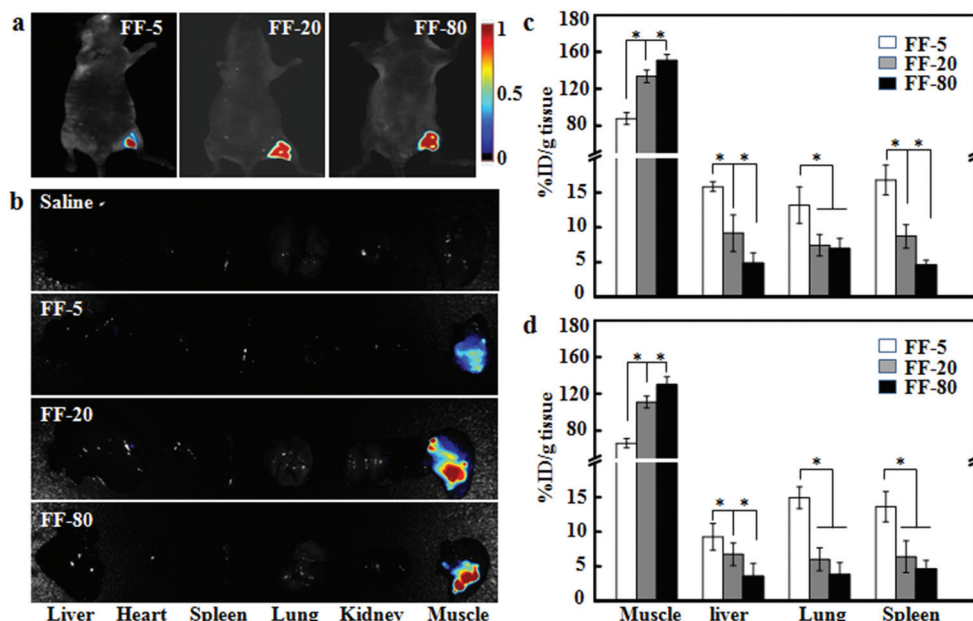


Fig. 4 (a) Typical fluorescent images of nude mice after the intramuscular injection of FF-5, FF-20 and FF-80 fiber fragments into the left hindlimb for 7 days. (b) Typical fluorescent images of liver, heart, spleen, lung, kidney, and quadriceps muscles retrieved from nude mice after the intramuscular injection of FF-5, FF-20 and FF-80 fiber fragments, compared with saline treatment. (c) The percentage of injected dose in per gram of quadriceps muscles, liver, lung, and spleen (%ID per g tissue) after intramuscular injection of fragmented PS/C6 fibers of FF-5, FF-20 and FF-80 for 7 and (d) for 28 days ($n = 4$, * $p < 0.05$).

3.5. Improvement of ischemic limb salvages after treatment

PAD is a severe medical condition associated with an obstruction of blood vessels due to atherosclerosis, stenosis, and embolism, which often leads to the loss of limbs or even life.³⁹ Fig. 5a shows the mouse images before and after treatment with different schedules for 4 weeks. The ischemia model was successfully established in hindlimbs, indicating significant changes in the color of toes and apparent cyanosis due to the oxygen shortage in the lower extremities. Extensive limb losses and foot necroses were observed for mice after treatment with saline, FF and FF + A/F, due to the lack of blood perfusion. The implantation of EF – A/F fibers and the local injection of AT-loaded and FA-loaded fiber fragments led to a better recovery of ischemia. Some necrotic toes were observed in mice after the implantation of EF – A/F fibers, while the necrosis was significantly retarded after local injection of FF – A/F fiber fragments, indicating a similar profile to normal limbs.

The therapeutic efficacy of drug-loaded fiber fragments was quantified by evaluating the physiological status of ischemic limbs by rating in three levels: limb salvage, foot necrosis, and limb loss.²⁸ As shown in Fig. 5b, compared with treatment with saline, FF and FF + A/F, intramuscular injection of drug-loaded fiber fragments and subcutaneous implantation of EF

– A/F fibers significantly reduced the percentage of limb loss. Compared with the saline group, the treatment with drug-loaded fiber fragments resulted in an increased percentage of limb salvages from 0 to 70% and a decreased percentage of limb losses from 80% to 10%. However, mice treated with FF or FF + A/F showed substantial limb losses from 70% to 80% and foot necroses at around 20%. In addition, a higher percentage of limb salvages of 70% was achieved after injection of FF – A/F fiber fragments compared with that after subcutaneous implantation of EF – A/F fibers at 40%.

3.6. Blood perfusion rate and TTC staining of ischemic muscles

Blood perfusion rate can reflect the blood flow recovery of ischemic limbs directly.³² In order to estimate the recovery of blood flow, the perfusion ratios were calculated using an LDP monitor immediately after the establishment of the hindlimb ischemia model and after treatments with different schedules. As shown in Fig. 6a, there was a significant decrease in the blood perfusion in the ischemic hindlimbs at 0.14 ± 0.02 after

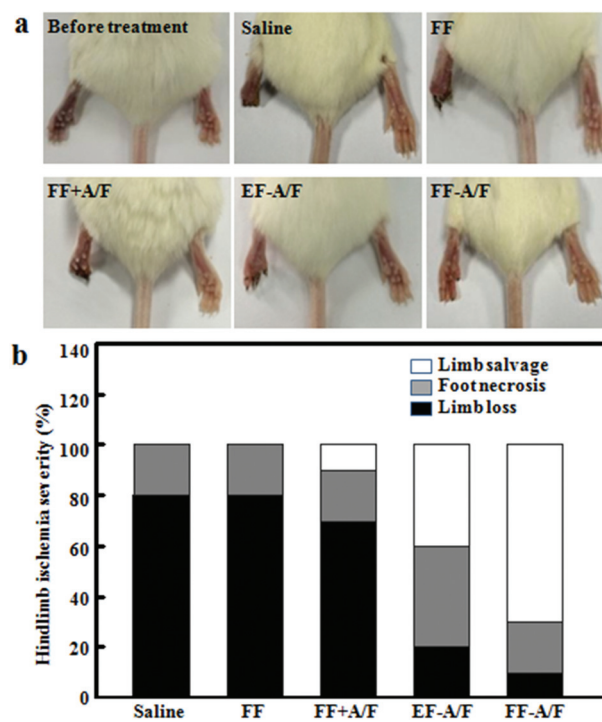


Fig. 5 (a) Intramuscular injection of the mixtures of AT-loaded and FA-loaded fragmented fibers (FF – A/F) and the implantation of electrospun fibers with loaded AT and FA (EF – A/F) improve recovery after hindlimb ischemia after 4 weeks, compared with the intramuscular injection of saline, fragmented fibers without drug entrapment (FF), and mixtures of fragmented fibers with free AT and FA (FF + A/F). (b) Percent of ischemic mice with limb salvages, foot necroses, and limb losses after different treatment schedules for 4 weeks ($n = 10$).

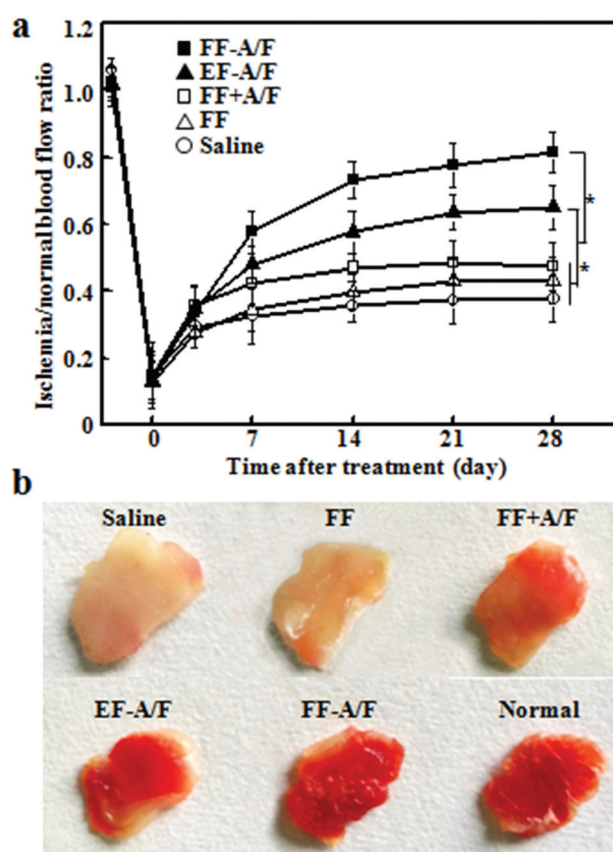


Fig. 6 (a) The blood flows of ischemic hindlimbs, measured using a laser Doppler perfusion monitor and compared with those of normal ones in the same animal, after intramuscular implantation of EF – A/F fibers and injection of FF – A/F, FF + A/F, and FF fiber fragments, using saline injection as the control ($n = 6$, * $p < 0.05$). (b) Typical staining images by 2,3,5-triphenyltetrazolium chloride of quadriceps muscles retrieved from ischemic hindlimbs after treatment for 4 weeks.

ligations of the femoral arteries, confirming the successful induction of severe limb ischemia. The perfusion ratio indicated a slight increase in the control group and no more changes during the following incubation, due to the angiogenesis induced by the oxygen-deficient environment in the tissues.⁴⁰ Similar profiles were observed for mice treated with fragmented fibers in the whole period. The inoculation of free drug with fragmented fibers led to a higher blood perfusion rate during 1 week, due to the synergistic effect of FA and AT.⁴¹ However, after 28 days of treatment, the perfusion ratio reached 0.43 ± 0.06 and 0.47 ± 0.07 for FF and FF + A/F groups, respectively, and there was no significant difference between them ($p > 0.05$). The sustained release of AT and FA enhanced the recovery of hindlimb ischemia, resulting in a significantly higher perfusion ratio of 0.65 ± 0.06 after the subcutaneous implantation of EF – A/F fibers for 28 days, compared with FF + A/F treatment ($p < 0.05$). In addition, the perfusion ratio of ischemic hindlimbs increased to 0.81 ± 0.06 after treatment with FF – A/F fiber fragments for 28 days, which was significantly higher than that of the EF – A/F group ($p < 0.05$).

TTC staining can be used to evaluate the ischemia situation from a macroscopic view, wherein pale tissues were observed in ischemic areas.³¹ As shown in Fig. 6b, muscles harvested from the ischemic limbs showed more viable tissues in the FF – A/F group, which resembled the appearance of normal muscles.

3.7. Muscle degeneration and fibrosis in ischemic hindlimbs

Ischemia usually causes the inflammation, degeneration and fibrosis of muscle tissues.⁴² Histological examinations of the ischemic hindlimbs were conducted to observe inflammation and fibrotic tissue formation in muscles after treatment. As shown in Fig. 7a, the invasion of granulocytes and macrophages indicated severe inflammation involved in the ischemic muscles after treatment with saline and fragmented fibers. However, few inflammatory cells were observed and less damaged muscles were evident in mice after treatment with drug-loaded fiber fragments.

Masson's Trichrome staining was performed to determine the fibrotic tissue formation in ischemic muscles. Fig. 7b shows the typical staining results of muscles retrieved after treatment with different schedules, wherein the blue regions indicate the formation of fibrotic tissues. Significant fibrosis was observed in the saline group and after treatment with fragmented fibers. However, few areas of fibrosis were detected in ischemic muscles after treatment with drug-loaded fiber fragments, indicating a staining profile similar to normal muscles. Fig. 7c summarizes the percentage of fibrosis, quantified by comparing the areas of fibrosis and muscles in the staining images. In the saline and FF groups, fibrotic tissues were observed in broad regions at the ratios of around 0.7% and over 0.6% after 7 and 28 days, respectively. Significant fibrotic tissues were also observed at the ratios of 0.4–0.5% after treatment with fragmented fibers and free drugs, even though they were reduced compared to those of saline control and FF groups. After treatment with EF – A/F fibers, fibrotic tissue for-

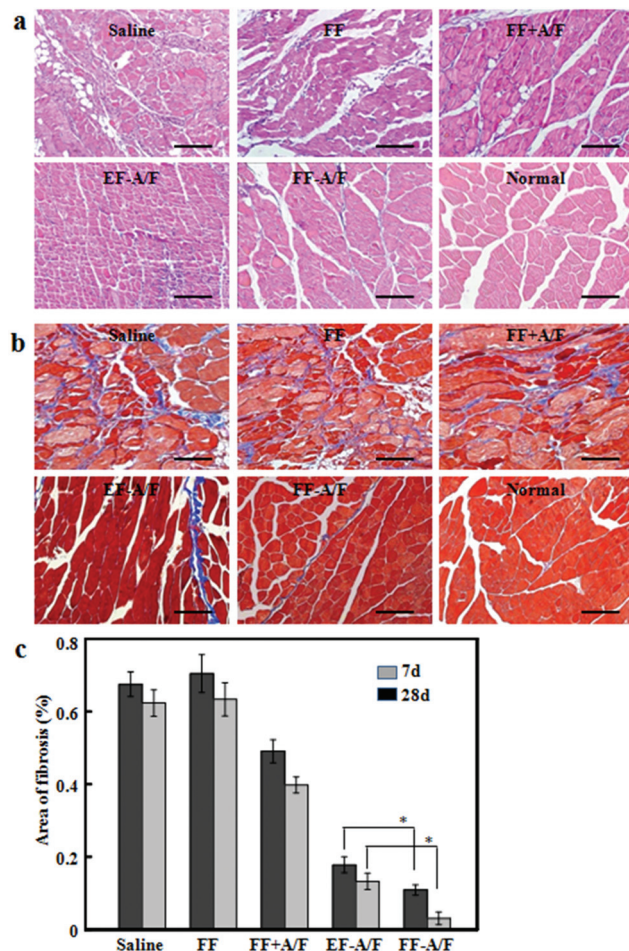


Fig. 7 (a) Typical HE staining images of quadriceps muscles retrieved from ischemic hindlimbs on day 7, and (b) Masson's Trichrome staining images on day 28 after intramuscular implantation of EF – A/F fibers and injection of FF – A/F, FF + A/F, and FF fiber fragments using saline injection and normal tissue as the control. Bars represent 200 μm . (c) The percentage of fibrosis in quadriceps muscles, quantified by comparing the areas of fibrosis (blue) and muscles (red) in Masson's Trichrome staining images, after different treatment schedules for 4 weeks ($n = 4$, $*p < 0.05$).

mation markedly decreased to $0.18 \pm 0.02\%$ and $0.13 \pm 0.02\%$ after 7 and 28 days, respectively. The percentages of fibrosis were $0.11 \pm 0.01\%$ after 7 days and $0.03 \pm 0.01\%$ after 28 days of treatment with FF – A/F fiber fragments, which were significantly lower than those of other groups ($p < 0.05$). These results indicated that the injection of drug-loaded fiber fragments protected limb muscles against muscle degeneration and fibrosis, with the maintenance of muscle fibril organization similar to that found in normal tissues.

3.8. Blood vessel formation in ischemic hindlimbs

The vascular density in ischemic tissues is an important indicator of angiogenesis.⁴² In the histological analysis, tissue sections were stained with anti-CD31 antibodies for ECs and anti-SMA antibodies for SMCs, respectively, to identify capillaries

and arterioles. As a transmembrane glycoprotein, CD31 is highly expressed in endothelium, and CD31 was used primarily to demonstrate the presence of ECs.⁴³ Fig. 8a shows the typical staining images of CD-31 on ischemic muscles after treatment for 28 days, and Fig. 8b summarizes the quantitative counts. The vessel densities in ischemic muscles in the control group was around 16 vessels per mm² after 7 days and indicated a slight increase to around 23 vessels per mm² after 28 days. The injection of fragmented fibers indicated no difference in the vessel density compared with the control ($p > 0.05$). The incubation of free drugs with fragmented fibers led to significantly higher vessel densities ($p < 0.05$), at around 29 and 37 vessels per mm² after 7 and 28 days, respectively. In addition, the sustained release of AT and FA from EF – A/F fibers after implantation enhanced the vessel formation in ischemic muscles, at around 54 and 77 vessels per mm² after 7 and 28 days, respectively. The injection of FF – A/F fiber fragments showed a significant increase in the vessel intensities to around 83 and 87 vessels per mm² after 7 and 28 days, respectively, which were significantly higher than those of other groups ($p < 0.05$).

The α -SMA expression is usually used to study the maturation levels of newly formed blood vessels.⁴⁴ Fig. 8c shows the typical staining images of α -SMA synthesis in ischemic muscles, suggesting the existence of α -SMA-expressing cells,

such as SMCs and pericytes, in the walls of newly formed vessels. The quantitative counts of the mature vessels are summarized in Fig. 8d, indicating a similar profile to CD-31 expression. The positively stained vessels were around 40 vessels per mm² after the subcutaneous implantation of EF – A/F fibers for 28 days, which was significantly higher than the control and FF groups ($p < 0.05$). Moreover, the injection of FF – A/F fiber fragments in the ischemic muscles led to the formation of mature vessels at a density of 47 vessels per mm², which was significantly higher than those of other groups ($p < 0.05$). The abovementioned results demonstrated an extensive microvessel formation after local injection of drug-loaded fiber fragments and no significant difference was found compared with normal tissues ($p > 0.05$).

As indicated above, the treatment with fragmented fibers with or without the inoculation of free drug indicated no significant effect on the ischemia recovery compared with saline treatment. The sustained release of FA and AT from electro-spun fibers attenuated tissue degeneration and restored the blood supply in the ischemic tissues. Compared with the subcutaneous implantation of EF – A/F fibers, the intramuscular injection of FF – A/F fiber fragments substantially reduced muscle degeneration with minimal fibrosis formation (Fig. 7), and significantly enhanced the neovessel formation (Fig. 8) and hindlimb perfusion in the ischemic tissues (Fig. 6), result-

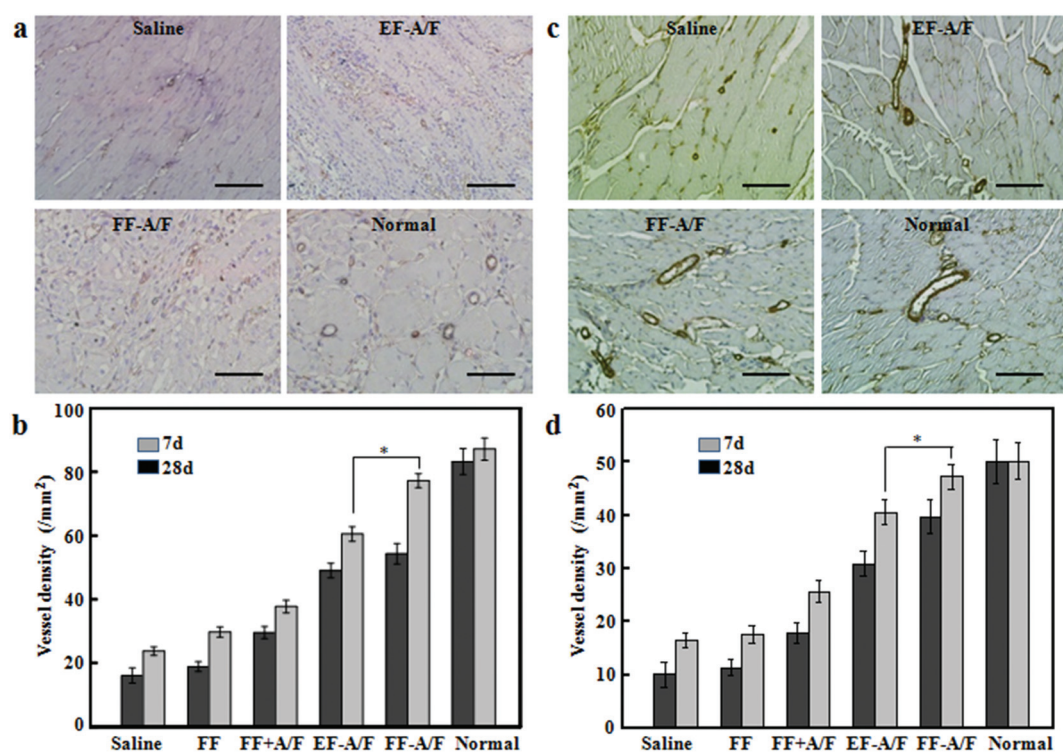


Fig. 8 Typical immunohistochemical staining images for (a) CD31 and (c) SMA syntheses in quadriceps muscles retrieved from ischemic hindlimbs after intramuscular implantation of EF – A/F fibers and injection of FF – A/F fiber fragments using saline injection and normal tissues as the control. Bars represent 200 μ m. Quantitative counts of (b) CD31 and (d) SMA-positive vessels and normalized to tissue areas (no. of vessels per mm²) after intramuscular implantation of EF – A/F fibers and injection of FF – A/F, FF + A/F, and FF fiber fragments for 7 and 28 days using saline injection as the control ($n = 4$. * $p < 0.05$).

ing in higher limb salvages (Fig. 5). The intramuscular injection allowed a regional distribution of fragmented fibers in ischemic tissues and an efficient attachment of ECs and SMCs recruited within them.⁴⁵ In addition, the distribution of fragmented fibers within tissues created more uniform dispersion of the released drugs and subsequently achieved an efficient synergistic promotion of blood vessel regeneration.

4. Conclusion

Fiber fragments were constructed by cryocutting aligned electrospun fibers, and the lengths were conveniently controlled by adjusting the slice thickness. FF-5, FF-20 and FF-80 fiber fragments showed no significant difference in the release profile for both AT and FA and in the promotion of cell proliferation and ECM syntheses. Compared with FF-5 and FF-80 fiber fragments, FF-20 achieved a good balance between the injectability and tissue retention after local injection into ischemic hindlimbs. Compared with the subcutaneous implantation of EF – A/F fibers, the intramuscular injection of drug-loaded fiber fragments substantially attenuated muscle degeneration with minimal fibrosis formation, significantly enhanced the neovessel formation and restoration of blood flows in the ischemic tissues, and efficiently promoted limb salvages with few limb losses. With their easy manipulation and lower invasiveness for *in vivo* administration, fragmented fibers should become potential drug carriers for disease treatment, wound recovery and tissue repair following local injection.

Acknowledgements

This study was supported by the National Natural Science Foundation of China (21274117 and 31470922), the Specialized Research Fund for the Doctoral Program of Higher Education (20120184110004), and the National Scientific and Technical Supporting Programs (2012BAI17B06).

Notes and references

- 1 A. Pacilli, G. Faggioli, A. Stella and G. Pasquinelli, *Ann. Vasc. Surg.*, 2010, **24**, 258–268.
- 2 B. H. Annex, *Nat. Rev. Cardiol.*, 2013, **10**, 387–396.
- 3 N. S. Bhise, R. B. Shmueli, J. C. Sunshine, S. Y. Tzeng and J. J. Green, *Expert Opin. Drug Delivery*, 2011, **8**, 485–504.
- 4 R. Madonna, D. A. Taylor, Y. J. Geng, R. De Caterina, H. Shelat, E. C. Perin and J. T. Willerson, *Circ. Res.*, 2013, **113**, 902–914.
- 5 T. M. Yau, C. Kim, G. Li, Y. Zhang, R. D. Weisel and R. K. Li, *Circulation*, 2005, **112**, 123–128.
- 6 Y. Imanishi, S. Miyagawa, N. Maeda, S. Fukushima, S. Kitagawa-Sakakida, T. Daimon, A. Hirata, T. Shimizu, T. Okano, I. Shimomura and Y. Sawa, *Circulation*, 2011, **124**, 10–17.
- 7 E. A. Phelps and A. J. Garcia, *Regener. Med.*, 2009, **4**, 65–80.
- 8 S. Kato, H. Amano, Y. Ito, K. Eshima, N. Aoyama, H. Tamaki, H. Sakagami, Y. Satoh, T. Izumi and M. Majima, *J. Pharmacol. Sci.*, 2010, **112**, 167–175.
- 9 H. Al Sabti, *J. Cardiothorac. Surg.*, 2007, **2**, 1–7.
- 10 J. Lee, S. H. Bhang, H. Park, B. S. Kim and K. Y. Lee, *Pharm. Res.*, 2010, **27**, 767–774.
- 11 H. Layman, M. G. Spiga, T. Brooks, S. Pham, K. A. Webster and F. M. Andreopoulos, *Biomaterials*, 2007, **28**, 2646–2654.
- 12 J. C. Chappell, J. Song, C. W. Burke, A. L. Klibanov and R. J. Price, *Small*, 2008, **4**, 1769–1777.
- 13 N. L. Elstad and K. D. Fowers, *Adv. Drug Delivery Rev.*, 2009, **61**, 785–794.
- 14 J. Zhou, Y. Zhao, J. Wang, S. Zhang, Z. Liu, M. Zhen, Y. Liu, P. Liu, Z. Yin and X. Wang, *Sci. World J.*, 2012, **2012**, 1–8.
- 15 A. L. Daugherty, L. K. Rangell, R. Eckert, J. Zavala-Solorio, F. Peale and R. J. Mrsny, *Eur. J. Pharm. Biopharm.*, 2011, **78**, 289–297.
- 16 D. Y. Ko, U. P. Shinde, B. Yeon and B. Jeong, *Prog. Polym. Sci.*, 2013, **38**, 672–701.
- 17 M. Jiang, J. Yang, C. Zhang, B. Liu, K. Chan, H. Cao and A. Lu, *Planta Med.*, 2010, **76**, 2048–2064.
- 18 H. Wang, Y. Zhang, T. Xia, W. Wei, F. Chen, X. Guo and X. Li, *Mol. Pharm.*, 2013, **10**, 2394–2403.
- 19 A. Greiner and J. H. Wendorff, *Angew. Chem., Int. Ed.*, 2007, **46**, 5670–5703.
- 20 X. M. Deng, X. H. Li, M. L. Yuan, C. D. Xiong, Z. T. Huang, W. X. Jia and Y. H. Zhang, *J. Controlled Release*, 1999, **58**, 123–131.
- 21 G. C. Li, P. Yang, W. Qin, M. F. Maitz, S. Zhou and N. Huang, *Biomaterials*, 2011, **32**, 4691–4703.
- 22 Y. Weng, Q. Song, Y. Zhou, L. Zhang, J. Wang, J. Chen, Y. Leng, S. Li and N. Huang, *Biomaterials*, 2011, **32**, 1253–1263.
- 23 J. G. Chen, X. H. Li, W. G. Cui, C. Y. Xie, J. Zou and B. Zou, *Adv. Eng. Mater.*, 2010, **12**, 529–538.
- 24 Y. Q. Liu, M. Ding and B. J. Xu, *Acta Pharm. Sin.*, 2000, **35**, 544–546.
- 25 H. Peng, J. W. Fu and R. Y. Yu, *Mater. Med. Res.*, 2009, **20**, 2925–2927.
- 26 H. L. Alves, L. A. Dos Santos and C. P. Bergmann, *J. Mater. Sci.: Mater. Med.*, 2008, **19**, 2241–2246.
- 27 Y. Hamada, K. Gonda, M. Takeda, A. Sato, M. Watanabe, T. Yambe, S. Satomi and N. Ohuchi, *Blood*, 2011, **118**, 93–100.
- 28 S. J. Kim, I. Jun, D. W. Kim, Y. B. Lee, Y. J. Lee, J. H. Lee, K. D. Park, H. Park and H. Shin, *Biomacromolecules*, 2013, **14**, 4309–4319.
- 29 V. Procházka, J. Gumulec, J. Chmelová, P. Klement, G. L. Klement, T. Jonszta, D. Černý and J. Krajca, *Vnitr. Lek.*, 2009, **55**, 173–178.
- 30 S. W. Cho, F. Yang, S. M. Son, H. J. Park, J. J. Green, S. Bogatyrev, Y. Mei, S. Park, R. Langer and D. G. Anderson, *J. Controlled Release*, 2012, **160**, 515–524.
- 31 F. Yang, S. W. Cho, S. M. Son, S. R. Bogatyrev, D. Singh, J. J. Green, Y. Mei, S. Park, S. H. Bhang, B. S. Kim,

- R. Langer and D. G. Anderson, *Proc. Natl. Acad. Sci. U. S. A.*, 2010, **107**, 3317–3322.
- 32 D. W. Kim, I. Jun, T. J. Lee, J. H. Lee, Y. J. Lee, H. K. Jang, S. Kang, K. D. Park, S. W. Cho, B. S. Kim and H. Shin, *Biomaterials*, 2013, **34**, 8258–8268.
- 33 F. Chen, H. Wan, T. Xia, X. Guo, H. Wang, Y. Liu and X. Li, *Eur. J. Pharm. Biopharm.*, 2013, **85**, 699–710.
- 34 A. S. Boehle, B. Sipos, U. Kliche, H. Kalthoff and P. Dohrmann, *Ann. Thorac. Surg.*, 2001, **71**, 1657–1665.
- 35 Y. Yang, X. H. Li, L. Cheng, S. H. He, J. Zou, F. Chen and Z. Zhang, *Acta Biomater.*, 2011, **7**, 2533–2543.
- 36 L. Whitehead, J. H. Collett and J. T. Fell, *Int. J. Pharm.*, 2000, **210**, 45–49.
- 37 C. M. Kelleher, S. E. McLean and R. P. Mecham, *Curr. Top. Dev. Biol.*, 2004, **62**, 153–188.
- 38 C. Adelow, T. Segura, J. A. Hubbell and P. Frey, *Biomaterials*, 2008, **29**, 314–326.
- 39 M. Fujihara, M. Fukata, K. Odashiro, T. Maruyama, K. Akashi and Y. Yokoi, *Angiology*, 2013, **64**, 112–118.
- 40 H. Song, S. Liu, C. Li, Y. Geng, G. Wang and Z. Gu, *Int. J. Nanomed.*, 2014, **9**, 3439–3452.
- 41 L. Yang, W. Y. Dou, T. Liu and D. W. Chin, *J. Exp. Tradit. Med. Formulae.*, 2008, **14**, 51–54.
- 42 J. Yamaguchi, K. F. Kusano, O. Masuo, A. Kawamoto, M. Silver, S. Murasawa, M. Bosch-Marce, H. Masuda, D. W. Losordo, J. M. Isner and T. Asahara, *Circulation*, 2003, **107**, 1322–1328.
- 43 A. P. Taylor, M. Rodriguez, K. Adams, D. M. Goldenberg and R. D. Blumenthal, *Int. J. Cancer*, 2003, **105**, 158–164.
- 44 G. D. Yancopoulos, S. Davis, N. W. Gale, J. S. Rudge, S. J. Wiegand and J. Holash, *Nature*, 2000, **407**, 242–248.
- 45 R. Ravichandran, J. R. Venugopal, S. Sundarrajan, S. Mukherjee, R. Sridhar and S. Ramakrishna, *Nanotechnology*, 2012, **23**, 1–14.